

A single TeV-scale scalar leptoquark in SO(10) grand unification and B-decay anomalies

Ufuk Aydemir,^a Tanumoy Mandal^{b,c} and Subhadip Mitra^d

^a*School of Physics, Huazhong University of Science and Technology, Wuhan, Hubei 430074, P. R. China*

^b*Department of Physics and Astronomy, Uppsala University, Box 516, SE-751 20 Uppsala, Sweden*

^c*Department of Physics and Astrophysics, University of Delhi, Delhi 110 007, India*

^d*Center for Computational Natural Sciences and Bioinformatics, International Institute of Information Technology, Hyderabad 500 032, India*

E-mail: uaydemir@hust.edu.cn, tanumoy.mandal@physics.uu.se,
subhadip.mitra@iiit.ac.in

ABSTRACT: One of the explanations proposed for the recent rare B -decay anomalies is the existence of a scalar leptoquark. We investigate a grand unification scenario where a single, charge $-1/3$ scalar leptoquark (S_1) is present as the only new physics candidate at the TeV-scale. This leptoquark along with the Standard Model (SM) Higgs doublet originates from the 10-dimensional real scalar multiplet in SO(10) grand unification framework. An S_1 residing in the same representation as the SM Higgs motivates the idea that its mass is close to the electroweak scale as the peculiar mass splittings within this multiplet do not occur. Therefore, possible detection of a TeV-scale S_1 leptoquark, unaccompanied by any other new particles, could be interpreted in favour of SO(10) grand unification. We explicitly show how the gauge coupling unification is achieved with only one intermediate symmetry breaking scale at which the Pati-Salam gauge group, obtained from the SO(10) breaking at the unification scale, is broken into the SM group. We investigate the phenomenological implications of our scenario and show that an S_1 with a specific Yukawa texture can still be a viable candidate to explain the $R_{D^{(*)}}$ anomalies. In order to obtain the allowed parameter space of our scenario, we consider the relevant flavour data including $R_{D^{(*)}}$ and $R_K^{\nu\nu}$ measurements, $Z \rightarrow \tau\tau$ decay and the latest $\tau\tau$ resonance search data at the LHC. We find that the LHC data strongly constrain the S_1 parameter space. We also find that there exist parts of parameter space where a single S_1 can still explain the $R_{D^{(*)}}$ anomalies without being in conflict with any of these constraints.

KEYWORDS: B -decay anomaly, scalar leptoquarks, SO(10) grand unification, LHC

Contents

1	Introduction	1
2	The SO(10) model	3
3	Gauge coupling unification	5
3.1	One-loop RG running	6
3.2	Unification with a single intermediate scale	8
4	Low energy phenomenology	10
4.1	The S_1 model	10
4.2	$R_{D^{(*)}}$ with S_1	11
4.3	Constraint from $R_K^{\nu\nu}$	12
4.4	Constraint from $Z \rightarrow \tau\tau$ decay	13
4.5	LHC Phenomenology and constraints	13
4.5.1	Decay modes of S_1	13
4.5.2	Production of S_1	13
4.5.3	Constraints from the LHC	15
4.6	Parameter scan	16
5	Discussion and conclusions	19

1 Introduction

During the past few years, several disagreements between experiments and the Standard Model (SM) predictions in rare B -decays have been reported by the Babar [1, 2], LHCb [3–7] and Belle [8–11] collaborations. So far, these anomalies have been quite persistent. The most significant ones have been observed in the $R_{D^{(*)}}$ and $R_{K^{(*)}}$ observables, defined as,

$$R_{D^{(*)}} = \frac{\text{BR}(B \rightarrow D^{(*)}\tau\nu)}{\text{BR}(B \rightarrow D^{(*)}\ell\nu)} \quad \text{and} \quad R_{K^{(*)}} = \frac{\text{BR}(B \rightarrow K^{(*)}\mu^+\mu^-)}{\text{BR}(B \rightarrow K^{(*)}e^+e^-)}. \quad (1.1)$$

Here, $\ell = \{e \text{ or } \mu\}$ and BR stands for branching ratio. The experimental values of R_D and R_{D^*} are in excess of their SM predictions [12–15] by 2.3σ and 3.0σ , respectively, based on the world averages as of summer 2018, according to the Heavy Flavor Averaging Group [16], whereas, the observed R_K and R_{K^*} are both suppressed compared to their SM predictions [17, 18] by $\sim 2.6\sigma$.

One of the possible explanations for the B -decay anomalies is the existence of scalar leptoquarks whose masses are in the few TeV range [19–52])¹. Leptoquarks, which posses

¹See some Refs. [53–59] for the vector-leptoquark solutions proposed to explain the B -decay anomalies.

both lepton and quark couplings, often exist in the Grand Unified Theories (GUTs) or in the Pati-Salam-type models. Considering that the LHC searches, except for these anomalies, have so far returned empty-handed, if the leptoquarks indeed turn out to be behind these anomalies, it is likely that there will be only a small number of particles to be discovered. However, their existence in small numbers at the TeV-scale would be curious in terms of its implications regarding physics beyond the Standard Model (BSM). Scalars in these models mostly come in large multiplets and it would be peculiar that only one or few of the components become light at the TeV-scale while others remain heavy. This is actually a well-speculated subject in the literature as the issue behind the infamous doublet-triplet splitting problem in supersymmetric theories and GUTs. In this context, even the SM Higgs in a GUT framework is troublesome if it turns out to be the only scalar at the electroweak scale.

In this paper, we consider a single scalar leptoquark, $S_1(\bar{3}, 1, 1/3)$, at the TeV-scale, in SO(10) GUT framework [60–73]. This particular leptoquark has been discussed in the literature to be responsible for one (or possibly both) of these B -decay anomalies [21, 22, 25, 32]. Furthermore, it is contained in a relatively small multiplet that resides in the fundamental representation of SO(10) group, a real $\mathbf{10}$, together with a scalar doublet with the quantum numbers that allow it to be identified as the SM Higgs. Therefore, the leptoquark is the only light scalar entity other than the SM Higgs doublet is justified in this scenario. A future discovery of such a leptoquark at the TeV-scale could be interpreted as an evidence in favour of an SO(10) GUT.

It has been argued in the literature that a real $\mathbf{10}_H$ in the minimal SO(10) set-up (together with a real $\mathbf{120}_H$ or a complex $\mathbf{120}_H$) is not favoured in terms of a realistic Yukawa sector [66]. On the other hand, it has been recently discussed in Ref. [73] that a Yukawa sector consisting of a real $\mathbf{10}_H$, a real $\mathbf{120}_H$ and a complex $\mathbf{126}_H$, can establish a realistic Yukawa sector due to the contributions from the scalars whose quantum numbers are the same as the SM Higgs doublet. Thus, this is the scalar content we assign in our model for the Yukawa sector.

Light colour triplets, similar to the one we consider in this paper, are oftentimes dismissed for the sake of proton stability since these particles in general have right quantum numbers for them to couple potentially dangerous operators that mediate proton decay. On the other hand, the proton stability could possibly be ensured through various symmetry mechanisms such as utilization of Peccei–Quinn (PQ) symmetry [66, 74], other U(1) symmetries such as the one discussed in Ref. [75], or a discrete symmetry similar to the one considered in Ref. [22]. Operators leading to proton decay could also be suppressed by a mechanism such as the one discussed in Ref. [76] or they could be completely forbidden by geometrical reasons [38]. In this work, in order not to contradict experimental evidence, we turn off the relevant couplings of S_1 which would lead to proton decay. However, we do not address possible underlying reasons behind the suppression or the elimination of these terms.

Inclusion of S_1 in the particle content of the model at the TeV-scale does not improve the status of the SM in term of gauge coupling unification, which cannot be realized by the particle content in question. Fortunately, in the SO(10) framework, there are other

ways to unify the gauge coupling constants, in contrast to models based on SU(5) group which also contains such a leptoquark within the same multiplet as the SM Higgs. As we illustrate in this paper, inserting a single intermediate phase where the active gauge group is the Pati-Salam group, $SU(4)_C \otimes SU(2)_L \otimes SU(2)_R$, which appears to be the favoured route of symmetry breaking by various phenomenological bounds [69], establishes coupling unification as desired. In our model, the Pati-Salam group is broken into the SM gauge group at an intermediate energy scale M_C , while SO(10) is broken into the Pati-Salam group at the unification scale M_U . We consider two versions of this scenario, depending on whether the left-right symmetry, so-called D -parity, is broken together with SO(10) at M_U , or it is broken at a later stage, at M_C , where the Pati-Salam symmetry is broken into the SM gauge symmetry.

After motivating the existence of a single TeV-scale S_1 from the SO(10) GUT framework, we move on to investigate the phenomenological implications of our model in this paper. In Ref. [22], it was shown that a TeV-scale S_1 leptoquark can explain the $R_{D^{(*)}}$ anomalies while simultaneously inducing the desired suppression in $R_{K^{(*)}}$ through box-diagrams. Since the most significant anomalies are seen in the $R_{D^{(*)}}$ observables, in this paper, we concentrate mostly on scenarios that can accommodate these observables. Generally, a TeV-scale S_1 requires one Yukawa coupling to be large to accommodate the $R_{D^{(*)}}$ anomalies [32, 45]. This, however, could create a problem for the $b \rightarrow s\bar{\nu}\nu$ transition rate measured in the $R_K^{\nu\nu}$ observable. In the SM, this decay proceeds through a loop whereas S_1 can contribute at the tree-level in this transition. Therefore, the measurements of $R_K^{\nu\nu}$ is very important to restrict the parameter space of S_1 .² Some specific Yukawa couplings of S_1 are also severely constrained from the $Z \rightarrow \tau\tau$ decay [47] and the LHC $\tau\tau$ resonance search data [48]. Therefore, it is evident that in order to find the $R_{D^{(*)}}$ -favoured parameter space while successfully accommodating other relevant constraints, one has to introduce new degrees of freedom in terms of new couplings and/or new particles. Here, we consider a specific Yukawa texture with three free couplings to show that a TeV-scale S_1 , consistent with relevant measurements, can still explain the $R_{D^{(*)}}$ anomalies.

The rest of the paper is organized as follows. In section 2, we introduce our model. In section 3, we display unification of the couplings for two versions of our model. In section 4, we present the related LHC phenomenology with a single extra leptoquark S_1 . We display the exclusion limits from the LHC data and discuss related future prospects. Finally in section 5, we end our paper with discussion and conclusions.

2 The SO(10) model

In our SO(10) model, we entertain the idea that the SM Higgs doublet is not the only scalar multiplet at the TeV-scale, but it is accompanied by a leptoquark $S_1 = (\bar{3}, 1, 1/3)$, both of which reside in a real 10-dimensional representation, $\mathbf{10}$, of SO(10) group. The

²One can avoid this conflict by introducing some additional degrees of freedom, as shown in Ref. [30]. Here, the authors have introduced an S_3 leptoquark in addition to the S_1 to concomitantly explain $R_{D^{(*)}}$ and $R_{K^{(*)}}$ while being consistent with $R_K^{\nu\nu}$.

peculiar mass splitting among the components of this multiplet does not occur, leading to a naturally light scalar leptoquark at the TeV-scale.

We start with a real $\mathbf{10}_H$ of $\text{SO}(10)$ whose Pati-Salam and the SM decompositions are given as

$$\begin{aligned} \mathbf{10} &= (1, 2, 2)_{422} \oplus (6, 1, 1)_{422} \\ &= \underbrace{\left(1, 2, \frac{1}{2}\right)_{321}}_H \oplus \underbrace{\left(1, 2, -\frac{1}{2}\right)_{321}}_{H^*} \oplus \underbrace{\left(3, 1, -\frac{1}{3}\right)_{321}}_{S_1^*} \oplus \underbrace{\left(\bar{3}, 1, \frac{1}{3}\right)_{321}}_{S_1}, \end{aligned} \quad (2.1)$$

where subscripts denote the corresponding gauge group and we set $Q = I_3 + Y$.

The scalar content we assign for the Yukawa sector consists of a real $\mathbf{10}_H$, a real $\mathbf{120}_H$, and a complex $\mathbf{126}_H$, which establishes a realistic Yukawa sector through mixing between the scalars whose quantum numbers are the same as the SM Higgs doublet, as shown in Ref. [73]. Note that

$$\mathbf{16} \otimes \mathbf{16} = \mathbf{10}_s \oplus \mathbf{120}_a \oplus \mathbf{126}_s, \quad (2.2)$$

where $\mathbf{16}$ is the spinor representation in which each family of fermions, including the right handed neutrino, resides in. The subscripts s and a denote the symmetric and anti-symmetric components. The Pati-Salam decompositions of $\mathbf{120}$ and $\mathbf{126}$ are given as

$$\begin{aligned} \mathbf{120} &= (1, 2, 2)_{422} \oplus (1, 1, 10)_{422} \oplus (1, 1, \bar{10})_{422} \oplus (6, 3, 1)_{422} \oplus (6, 1, 3)_{422} \oplus (15, 2, 2)_{422}, \\ \mathbf{126} &= (10, 3, 1)_{422} \oplus (\bar{10}, 1, 3)_{422} \oplus (15, 2, 2)_{422} \oplus (6, 1, 1)_{422}. \end{aligned} \quad (2.3)$$

The Yukawa terms are then given as

$$\mathcal{L}_Y = \mathbf{16}_F (Y_{10} \mathbf{10}_H + Y_{120} \mathbf{120}_H + Y_{126} \bar{\mathbf{126}}_H) \mathbf{16}_F + h.c., \quad (2.4)$$

where Y_{10} and Y_{126} are complex Yukawa matrices, symmetric in the generation space, and Y_{120} is a complex anti-symmetric one.

For the symmetry breaking pattern, we consider a scenario in which the intermediate phase has the gauge symmetry of the Pati-Salam group $\text{SU}(4)_C \otimes \text{SU}(2)_L \otimes \text{SU}(2)_R$. Note that this specific route of symmetry breaking appears to be favoured by various phenomenological bounds [69]. We consider two versions of this scenario depending on whether or not the Pati-Salam gauge symmetry is accompanied by the D -parity invariance, a \mathbb{Z}_2 symmetry that maintains the complete equivalence of the left and the right sectors [63, 64, 77], after the $\text{SO}(10)$ breaking. The symmetry breaking sequence is schematically given as

$$\text{SO}(10) \xrightarrow[\langle \mathbf{210} \rangle \text{ (or } \langle \mathbf{54} \rangle)]{M_U} G_{422} \text{ (or } 422D) \xrightarrow[\langle \mathbf{126} \rangle]{M_C} G_{321} \text{ (SM)} \xrightarrow[\langle \mathbf{10} \rangle]{M_Z} G_{31}, \quad (2.5)$$

where, we use the notation,

$$G_{422D} \equiv \text{SU}(4)_C \otimes \text{SU}(2)_L \otimes \text{SU}(2)_R \otimes D,$$

$$\begin{aligned}
G_{422} &\equiv \text{SU}(4)_C \otimes \text{SU}(2)_L \otimes \text{SU}(2)_R , \\
G_{321} &\equiv \text{SU}(3)_C \otimes \text{SU}(2)_L \otimes \text{U}(1)_Y , \\
G_{31} &\equiv \text{SU}(3)_C \otimes \text{U}(1)_Q .
\end{aligned}
\tag{2.6}$$

The first stage of the spontaneous symmetry breaking occurs through the Pati-Salam singlet in the $\text{SO}(10)$ multiplet **210**, acquiring a vacuum expectation value (VEV) at the unification scale M_U . This singlet is odd under D -parity and, therefore, the resulting symmetry group is G_{422} in the first stage of the symmetry breaking. In the second step, the breaking of G_{422} into the SM gauge group G_{321} is realized through the SM-singlet contained in $\Delta_R(\overline{10}, 1, 3)_{422}$ of **126**, acquiring VEV at the energy scale M_C , which also yields a Majorana mass for the right-handed neutrino. The last stage of the symmetry breaking is realized predominantly through the SM doublet contained in $\phi(1, 2, 2)_{422}$ of **10**. This doublet is mixed with other doublets contained in $\phi(1, 2, 2)_{422}$ and $\Sigma(15, 2, 2)_{422}$ of the real multiplet **120** and $\Sigma(15, 2, 2)_{422}$ of **126**, which yields a realistic Yukawa sector, consistent with the observed fermion masses [73]. The mass-scale of these Pati-Salam multiplets is set as M_C , the energy scale at which the Pati-Salam symmetry is broken into the SM, while the rest of the fields are assumed to be heavy at the unification scale M_U . The only degrees of freedom, assumed to survive down to the electroweak scale, are the SM Higgs doublet and the colour triplet, S_1 . We call this model A_1 .

In the second scenario, which we call model A_2 , the first stage of the symmetry breaking is realized through the Pati-Salam singlet contained in **54**, acquiring a VEV. This singlet is even under D -parity, and therefore, D -parity is not broken at this stage with the $\text{SO}(10)$ symmetry, and the resulting symmetry group valid down to M_C is G_{422} . The rest of the symmetry breaking continues in the same way as in model A_1 . Consequently in model A_2 , we include one more Pati-Salam multiplet at M_C , $\Delta_L(10, 3, 1)$, in order to maintain a complete left-right symmetry down to M_C . The scalar content and, for the later use, the corresponding renormalization group (RG) coefficients in each energy interval are given in Table 1.

Finally, the relevant Lagrangian for phenomenological analysis at the low energy is given by

$$\mathcal{L} \supset (D_\mu S_1)^\dagger (D^\mu S_1) - M_{S_1}^2 |S_1|^2 - \lambda |S_1|^2 |H|^2 + (\mathbf{\Lambda}^L \bar{Q}^c i\tau_2 L + \mathbf{\Lambda}^R \bar{u}_R^c e_R) S_1^\dagger + h.c. \tag{2.7}$$

where Q and L are the SM quark and lepton doublets (for each family), $\mathbf{\Lambda}^{L/R}$ are coupling matrices in flavour space and $\psi^c = C\bar{\psi}^T$ are charge conjugate spinors. Inclusion of S_1 can affect the stability of electroweak vacuum via loop effects. The relevant discussion can be found in Ref. [78].

3 Gauge coupling unification

In this section, after we lay out preliminaries for one-loop RG running and show that the new particle content at the TeV-scale does not lead to unification of the SM gauge couplings directly, we illustrate gauge coupling unification with a single intermediate step of symmetry breaking. Once the particle content at low energies is determined, there may

Table 1. The scalar content and the RG coefficients in the energy intervals for model $A_{1,2}$. Note that the ϕ fields, the Φ field, and one of the Σ fields originate from real SO(10) multiplets and thus $\eta = 1/2$ condition should be employed when necessary while determining the RG coefficients in Eq. (3.2).

Interval	Scalar content for model A_1 (A_2)	RG coefficients
II	$\phi(1, 2, 2) \times 2, \Phi(6, 1, 1),$ $\Sigma(15, 2, 2) \times 2, \Delta_R(\overline{10}, 1, 3),$ (and $\Delta_L(10, 3, 1)$ for model A_2)	$[a_4, a_L, a_R] = \left[\frac{1}{2} \left(\frac{7}{2} \right), \frac{9}{2} \left(\frac{67}{6} \right), \frac{67}{6} \right]$
I	$H \left(1, 2, \frac{1}{2} \right), S_1 \left(\overline{3}, 1, \frac{1}{3} \right)$	$[a_3, a_2, a_1] = \left[\frac{-41}{6}, \frac{-19}{6}, \frac{125}{18} \right]$

be numerous ways to unify the gauge couplings, depending on selection of the scalar content in SO(10) representations. In the literature, the canonical way to make this selection is through adopting a minimalistic approach, allowed by the observational constraints. In the following, we pursue the same strategy while taking into account the analysis made in Ref. [73] for a realistic Yukawa sector.

3.1 One-loop RG running

For a given particle content, the gauge couplings in an energy interval $[M_A, M_B]$ evolve under one-loop RG running as

$$\frac{1}{g_i^2(M_A)} - \frac{1}{g_i^2(M_B)} = \frac{a_i}{8\pi^2} \ln \frac{M_B}{M_A}, \quad (3.1)$$

where the RG coefficients a_i are given by [79, 80]

$$a_i = -\frac{11}{3}C_2(G_i) + \frac{2}{3} \sum_{R_f} T_i(R_f) \cdot d_1(R_f) \cdots d_n(R_f) + \frac{\eta}{3} \sum_{R_s} T_i(R_s) \cdot d_1(R_s) \cdots d_n(R_s), \quad (3.2)$$

and the full gauge group is given as $G = G_i \otimes G_1 \otimes \dots \otimes G_n$. The summation in Eq. (3.2) is over irreducible chiral representations of fermions (R_f) and irreducible representations of scalars (R_s) in the second and the third terms, respectively. The coefficient η is either 1 or 1/2, depending on whether the corresponding representation is complex or (pseudo) real, respectively. $d_j(R)$ is the dimension of the representation R under the group $G_{j \neq i}$. $C_2(G_i)$ is the quadratic Casimir for the adjoint representation of the group G_i , and T_i is the Dynkin index of each representation. For U(1) group, $C_2(G) = 0$ and

$$\sum_{f,s} T = \sum_{f,s} Y^2, \quad (3.3)$$

where Y is the $U(1)_Y$ charge.

Representation	SU(2)	SU(3)	SU(4)
2	$\frac{1}{2}$	—	—
3	2	$\frac{1}{2}$	—
4	5	—	$\frac{1}{2}$
6	$\frac{35}{2}$	$\frac{5}{2}$	1
8	42	3	—
10	$\frac{165}{2}$	$\frac{15}{2}$	3
15	280	$10, \frac{35}{2}$	4

Table 2. Dynkin index T_i for various irreducible representations of SU(2), SU(3), and SU(4). Our normalization convention in this paper follows the one adopted in Ref. [80]. Notice that there are the two inequivalent 15 dimensional irreducible representations for SU(3).

Addition of S_1 to the particle content of the SM does not help in unifying the gauge couplings as displayed in Fig. 1, where the RG running is performed with the modified RG coefficients given in Table 1 in interval I, while interval II is irrelevant to this particular case. Unification of the gauge couplings can be established through intermediate symmetry breaking between the electroweak scale and unification scale, as we illustrate in the next subsection with a single intermediate step of symmetry breaking.

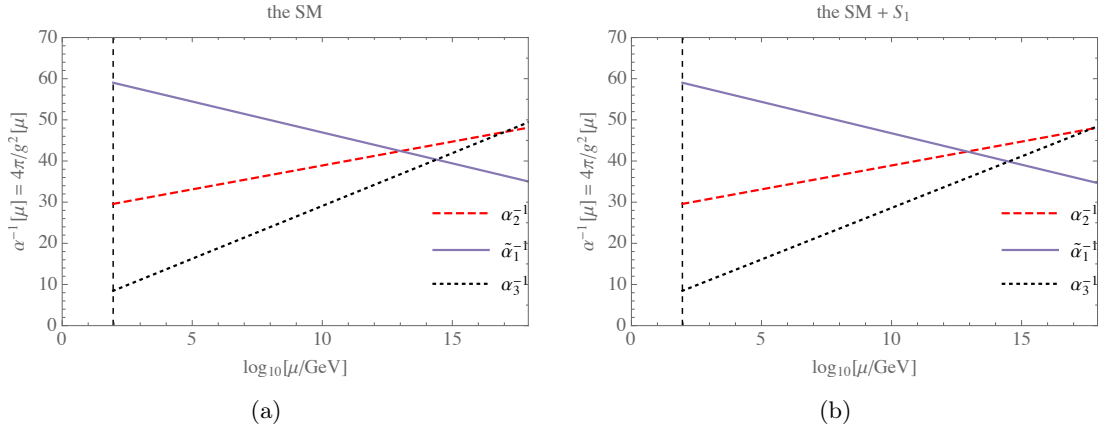


Figure 1. Running of the gauge couplings with the particle content of the SM and with inclusion of S_1 . The vertical dotted line correspond to the electroweak scale M_Z . For α_1^{-1} , we plot the redefined quantity $\tilde{\alpha}_1^{-1} \equiv \frac{3}{5}\alpha_1^{-1}$ as required by the SO(10) boundary conditions. Including the leptoquark in the particle content does not provide a significant modification to the SM RG running in favour of unification.

3.2 Unification with a single intermediate scale

We start with labeling the energy intervals in between symmetry breaking scales $[M_Z, M_C]$ and $[M_C, M_U]$ with Roman numerals as

$$\begin{aligned} \text{I} &: [M_Z, M_C], \quad G_{213} \text{ (SM)}, \\ \text{II} &: [M_C, M_U], \quad G_{224} \text{ or } G_{224D}. \end{aligned} \quad (3.4)$$

The boundary/matching conditions we impose on the couplings at the symmetry breaking scales are:

$$\begin{aligned} M_U &: g_L(M_U) = g_R(M_U) = g_4(M_U), \\ M_C &: g_3(M_C) = g_4(M_C), \quad g_2(M_C) = g_L(M_C), \\ &\quad \frac{1}{g_1^2(M_C)} = \frac{1}{g_R^2(M_C)} + \frac{2}{3} \frac{1}{g_4^2(M_C)}, \quad g_L(M_C) = g_R(M_C) \text{ (absent in the } G_{224} \text{ case)} \\ M_Z &: \frac{1}{e^2(M_Z)} = \frac{1}{g_1^2(M_Z)} + \frac{1}{g_2^2(M_Z)}. \end{aligned} \quad (3.5)$$

We use the central values of the low energy data as the boundary conditions in the RG running (in the $\overline{\text{MS}}$ scheme) are [81, 82] $\alpha^{-1} = 127.95$, $\alpha_s = 0.118$, $\sin^2 \theta_W = 0.2312$ at $M_Z = 91.2 \text{ GeV}$, which translate to $g_1 = 0.357$, $g_2 = 0.652$, $g_3 = 1.219$. The coupling constants are all required to remain in the perturbative regime during the evolution from M_Z to M_U .

The RG coefficients, a_i , differ depending on the particle content in each energy interval, changing every time symmetry breaking occurs. Together with the matching and boundary conditions, one-loop RG running leads to the following conditions on the symmetry breaking scales M_U and M_C :

$$\begin{aligned} 2\pi \left[\frac{3 - 8 \sin^2 \theta_W(M_Z)}{\alpha(M_Z)} \right] &= (3a_1 - 5a_2) \ln \frac{M_C}{M_Z} + (-5a_L + 3a_R + 2a_4) \ln \frac{M_U}{M_C}, \\ 2\pi \left[\frac{3}{\alpha(M_Z)} - \frac{8}{\alpha_s(M_Z)} \right] &= (3a_1 + 3a_2 - 8a_3) \ln \frac{M_C}{M_Z} + (3a_L + 3a_R - 6a_4) \ln \frac{M_U}{M_C}, \end{aligned} \quad (3.6)$$

where the notation on a_i is self-evident. The unified gauge coupling α_U at scale M_U is then obtained from

$$\frac{2\pi}{\alpha_U} = \frac{2\pi}{\alpha_s(M_Z)} - \left(a_4 \ln \frac{M_U}{M_C} + a_3 \ln \frac{M_C}{M_Z} \right). \quad (3.7)$$

Thus, once the RG coefficients in each interval are specified, the scales M_U and M_C , and the value of α_U are uniquely determined. The results are given in Table 3, and unification of the couplings is displayed in Fig. 2 for each model.

As mentioned previously, we assume in this paper that the proton-decay mediating couplings of S_1 are suppressed. On the other hand, we do not make any assumptions regarding the other potentially dangerous operators which could lead to proton decay.

Thus, it is necessary to inspect whether the predictions of our models displayed in Table 3 are compatible with the current bounds coming from the proton decay searches or not. The most recent and stringent bound on the lifetime of proton comes from the mode $p \rightarrow e^+\pi^0$, as $\tau_p > 1.6 \times 10^{34}$ years [83]. As for the proton decay modes that are mediated by the super-heavy gauge bosons, which reside in the adjoint representation of SO(10) **45**, considering that $\tau_p \sim M_U^4/m_p^5\alpha_U^2$ [84], we obtain $M_U \gtrsim 10^{15.9}$ GeV, which is consistent with predictions of both model A_1 and model A_2 , within an order of magnitude of the latter. Additionally, since M_C is the scale at which the Pati-Salam symmetry breaks into the SM, it determines the expected mass values for the proton-decay-mediating colour-triplets. From a naive analysis [69], it can be shown that the current bounds on the proton lifetime requires $M_C \gtrsim 10^{11}$ GeV, again consistent with the predictions of both model A_1 and model A_2 , within an order of magnitude of the former. Note that these bounds should be taken as order-of-magnitude estimates since, while obtaining them, we approximate the anticipated masses of the super-heavy gauge bosons and the colour-triplets as $M_X \sim M_U$ and $M_T \sim M_C$, while it would not be unreasonable to expect that these mass values could differ from the corresponding energy scales within an order of magnitude.

Model	A_1	A_2
$\log_{10}(M_U/\text{GeV})$	17.1	15.6
$\log_{10}(M_C/\text{GeV})$	10.9	13.7
α_U^{-1}	29.6	35.4

Table 3. The predictions of models A_1 and A_2 .

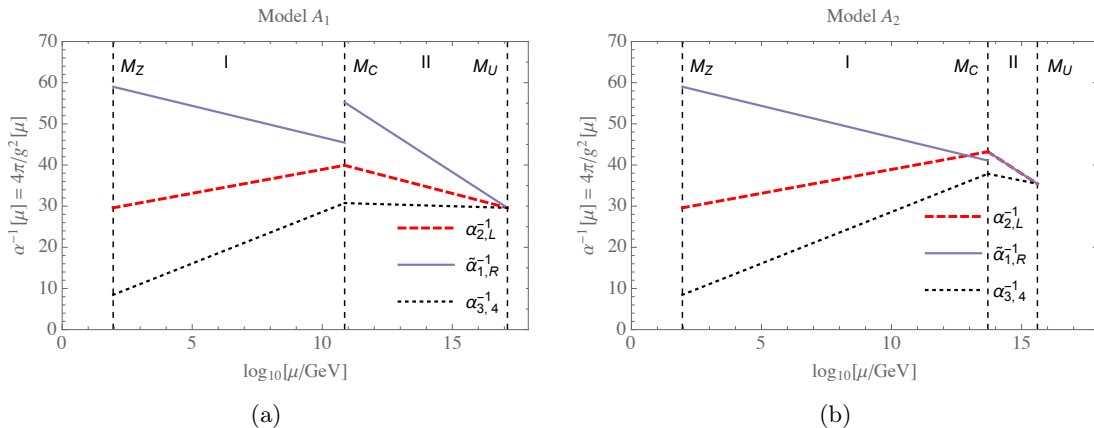


Figure 2. Running of the gauge couplings for models A_1 and A_2 . Note that $\tilde{\alpha}_1^{-1} \equiv \frac{3}{5}\alpha_1^{-1}$. The discontinuity at M_C in each plot is consistent with the boundary conditions given in Eq. (3.5).

4 Low energy phenomenology

Existence of a TeV-scale charge $-1/3$ scalar leptoquark (normally denoted as S_1) in a GUT framework is very interesting from a phenomenological perspective mainly because of two reasons. First, its existence is testable at the LHC. The direct detection searches for scalar leptoquarks have been putting exclusion bounds on S_1 [85, 86] with different decay hypotheses. Second, as mentioned earlier, such a leptoquark can offer an explanation of some persistent flavour anomalies observed in several experiments. For example, if we consider the anomalies observed in the B -meson semileptonic decays via charged current (collectively these show the most significant departure from the SM expectations), S_1 can provide an explanation if it couples with τ and neutrino(s) and b - and c -quarks. The direct LHC bounds on such a leptoquark is not very severe but as it has been pointed out in Ref. [48], the present LHC data in the $pp \rightarrow \tau\tau/\tau\nu$ channels have actually put some constraints in the S_1 parameter space relevant for explaining the observed $R_{D^{(*)}}$ anomalies. Here, using flavour data and LHC constrains, we obtain the allowed parameter space of our model. We also point out some possible new search channels at the LHC. On the flavour side, our primary focus, in this paper, is on the charged current anomalies observed in the semileptonic B -decays in the $R_{D^{(*)}}$ observables and hence, we would mostly rely on Ref. [48] for the LHC bounds. For simplicity, we focus only on the interaction terms of S_1 that could play role to address the $R_{D^{(*)}}$ anomalies.

4.1 The S_1 model

The single TeV-scale S_1 leptoquark that originates from the GUT model discussed in Section 2 transforms under the SM gauge group as $(\mathbf{3}, \mathbf{1}, -1/3)$. The low energy interactions of S_1 with the SM fields are shown in a compact manner in Eq. (2.7). Here, we display the relevant interaction terms for our phenomenological analysis,

$$\mathcal{L} \supset [\lambda_{ij}^L \bar{Q}_i^c (i\tau_2) L_j + \lambda_{ij}^R \bar{u}^c \ell_R] S_1^\dagger + h.c. , \quad (4.1)$$

where Q_i and L_i denote the i -th generation quark and lepton doublets, respectively and λ_{ij}^H represents the coupling of S_1 with a charge conjugate quark of i -th generation and a lepton of j -th generation with chirality H . Without any loss of generality, we assume all λ 's are real in our collider analysis since the LHC data that we consider are insensitive to their complex nature. Also, we only consider mixing among quarks and ignore neutrino mixing since all neutrino flavours contribute to the missing energy and hence not distinguishable at the LHC.

The couplings of S_1 to the first generation SM fermions are heavily constrained [32]. Hence, we assume $\lambda_{1i}, \lambda_{i1} = 0$ in our analysis.³ The parton level Feynman diagrams for the $b \rightarrow c\tau\nu$ decay (responsible for $B \rightarrow D^{(*)}\tau\nu$) are shown in Fig. 3. In order to have a nonzero contribution in the $R_{D^{(*)}}$ observables from S_1 , we need $b\nu S_1$ and $c\tau S_1$ couplings to be nonzero simultaneously. Minimally, one can start with just a single free coupling –

³However, these couplings can be generated through the Cabibbo-Kobayashi-Maskawa (CKM) mixing. We refer the interested readers to Ref. [32] for various important flavour constrains in this regard.

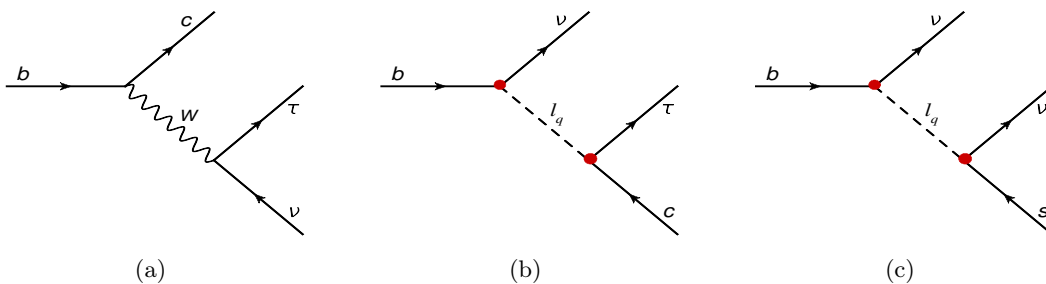


Figure 3. Leading order partonic level Feynman diagrams responsible for the $B \rightarrow D^{(*)}\tau\nu$ decay (a) in the SM, (b) in the S_1 model and (c) $B \rightarrow K\nu\nu$.

either λ_{23}^L or λ_{33}^L . The coupling λ_{23}^L (λ_{33}^L) directly generates $c\tau S_1$ ($b\nu S_1$) interaction and other one, i.e., the $b\nu S_1$ ($c\tau S_1$) can be generated through mixing among quarks. These two minimal scenarios are discussed in detail in Ref [48]. For these two cases, the Lagrangian in Eq. (4.1) can be written explicitly as,

$$C_1: \mathcal{L} \supset \lambda_{23}^L [\bar{c}^c \tau_L - (V_{cb}\bar{b}^c + V_{cs}\bar{s}^c + V_{cd}\bar{d}^c) \nu] S_1^\dagger + h.c. \quad (\lambda_{33}^L = 0), \quad (4.2)$$

$$C_2: \mathcal{L} \supset \lambda_{33}^L [(V_{ub}^* \bar{u}^c + V_{cb}^* \bar{c}^c + V_{tb}^* \bar{t}^c) \tau_L - \bar{b}^c \nu] S_1^\dagger + h.c. \quad (\lambda_{23}^L = 0). \quad (4.3)$$

There, it is shown that for C_1 , the $R_{D^{(*)}}$ favoured parameter space is already ruled out by the latest LHC data. On the other hand, C_2 is not seriously constrained by the data since the LHC is insensitive to the coupling λ_{33}^L . Only the pair production (insensitive to λ_{33}^L) of S_1 searches in the $t\tau\tau$ and $b\nu\nu$ modes exclude M_{S_1} up to 900 GeV [85] and 1100 GeV [86], respectively assuming 100% BR in the respective modes. However, in Ref. [47] it is shown that C_2 too is ruled out by the electroweak precision data on the $Z \rightarrow \tau\tau$ decay.

The above cases, C_1 and C_2 , are two extremes. One can consider a situation, where both λ_{23}^L and λ_{33}^L are nonzero to explain $R_{D^{(*)}}$ anomalies within the LHC bounds [48]. However, $B \rightarrow K\nu\nu$ decay results severely constrain such a scenario due to tree-level leptoquark contribution. In Refs. [32, 45], it is found that $\mathcal{O}(1)$ λ_{23}^R is required to explain various flavour anomalies simultaneously being consistent with other relevant experimental results.

In this paper, we allow all λ_{23}^L , λ_{33}^L and λ_{23}^R to be nonzero and perform a parameter scan for a single S_1 solution of the $R_{D^{(*)}}$ anomalies. We locate the $R_{D^{(*)}}$ favoured parameter space (that also somewhat accommodates $R_{K^{(*)}}$ anomalies) that satisfies the limits from $B \rightarrow K\nu\nu$ and $Z \rightarrow \tau\tau$ decays and is still allowed by the latest LHC data. An S_1 from this parameter space can provides new final states at the LHC viz. $\tau\tau + jets$ and $\tau + \cancel{E}_T + jets$ in which leptoquarks have not been searched before.

4.2 $R_{D^{(*)}}$ with S_1

In the SM, the semi-tauonic B -decay is mediated by the left-handed charged currents and the corresponding four-Fermi interactions are given by the following effective Lagrangian

$$\mathcal{L}_{\text{SM}} = -\frac{4G_F}{\sqrt{2}} V_{cb} [\bar{c}\gamma^\mu P_L b] [\bar{\tau}\gamma_\mu P_L \nu_\tau]. \quad (4.4)$$

In presence of new physics, there are total five four-Fermi operators that can appear in the effective Lagrangian of the $B \rightarrow D^{(*)}\tau\nu$ decay,

$$\mathcal{L} \supset -\frac{4G_F}{\sqrt{2}}V_{cb}[(1 + \mathcal{C}_{V_L})\mathcal{O}_{V_L} + \mathcal{C}_{V_R}\mathcal{O}_{V_R} + \mathcal{C}_{S_L}\mathcal{O}_{S_R} + \mathcal{C}_{S_R}\mathcal{O}_{S_R} + \mathcal{C}_{T_R}\mathcal{O}_{T_R}] , \quad (4.5)$$

where the \mathcal{C} 's are the Wilson coefficients associated with the following effective operators

- Vector operators: $\mathcal{O}_{V_L} = [\bar{c}\gamma^\mu P_L b][\bar{\tau}\gamma_\mu P_L \nu]$, $\mathcal{O}_{V_R} = [\bar{c}\gamma^\mu P_R b][\bar{\tau}\gamma_\mu P_L \nu]$
- Scalar operators: $\mathcal{O}_{S_L} = [\bar{c}P_L b][\bar{\tau}P_L \nu]$, $\mathcal{O}_{S_R} = [\bar{c}P_R b][\bar{\tau}P_L \nu]$
- Tensor operator: $\mathcal{O}_{T_L} = [\bar{c}\sigma^{\mu\nu} P_L b][\bar{\tau}\sigma_{\mu\nu} P_L \nu]$

The operator \mathcal{O}_{T_R} is identically zero. The S_1 leptoquark can generate only the $\mathcal{O}_{V_L, S_L, T_L}$ operators and the Wilson coefficients in terms of the S_1 parameters are given by,

$$\mathcal{C}_{V_L} = \frac{1}{2\sqrt{2}G_F V_{cb}} \frac{\lambda_{23}^{L*}\lambda_{33}^L}{2M_{S_1}^2}, \quad \mathcal{C}_{S_L} = \frac{1}{2\sqrt{2}G_F V_{cb}} \frac{\lambda_{33}^L\lambda_{23}^R}{2M_{S_1}^2}, \quad \mathcal{C}_{T_L} = -\frac{1}{4}\mathcal{C}_{S_L}. \quad (4.6)$$

Note that these coefficients are obtained at the mass scale M_{S_1} whereas the running of the strong coupling down to $m_b \sim 4.2$ GeV can change these coefficients substantially except \mathcal{C}_{V_L} which is protected by the Ward identity of quantum chromodynamics (QCD). The relation $\mathcal{C}_{T_L}(M_{S_1}) = -(1/4)\mathcal{C}_{S_L}(M_{S_1})$ is altered due to running coupling and we include this effect in our analysis by following the expressions in Ref. [32]. In terms of the Wilson coefficients, the $R_{D^{(*)}}$ looks like [35, 87],

$$R_{D^{(*)}} = \left(|1 + \mathcal{C}_{V_L}|^2 + \frac{1}{4}|\mathcal{C}_{S_L}|^2 + 12|\mathcal{C}_{T_L}|^2 \right) R_{D^{(*)}}^{SM}, \quad (4.7)$$

where, for simplicity, we have assumed that any momentum dependence in the form factors will not affect the $R_{D^{(*)}}/R_{D^{(*)}}^{SM}$ ratio drastically. For our convenience, we define the ratio, $r_{D^{(*)}} = R_{D^{(*)}}/R_{D^{(*)}}^{SM}$. Given the current experimental measurements and the SM determinations, we find the following 1σ allowed ranges for $r_{D^{(*)}}$,

$$r_D = 1.25 \pm 0.08, \quad r_{D^*} = 1.32 \pm 0.17. \quad (4.8)$$

4.3 Constraint from $R_K^{\nu\nu}$

The SM flavour changing neutral current $b \rightarrow s\bar{\nu}\nu$ transition proceeds through a loop and is suppressed by the Glashow-Iliopoulos-Maiani mechanism. Whereas in our model, S_1 can mediate this transition at the tree-level (see Fig. 3(c)). Therefore, this neutral current decay can heavily constrain the parameter space of our model. We define the following ratio,

$$R_K^{\nu\nu} = \frac{\Gamma(B \rightarrow K\nu\nu)}{\Gamma(B \rightarrow K\nu\nu)_{SM}} \quad (4.9)$$

According to Ref. [88], the upper limit of this ratio is, $R_K^{\nu\nu} < 4.3$ at 90% confidence limit (CL). In terms of our model parameters, $R_K^{\nu\nu}$ is given by the following expression,

$$R_K^{\nu\nu} = 1 - \frac{2a}{3M_{S_1}^2} \text{Re} \left(\frac{\lambda_{23}^{L*}\lambda_{33}^L}{V_{tb}V_{ts}^*} \right) + \frac{a^2}{3M_{S_1}^4} \left| \frac{\lambda_{23}^{L*}\lambda_{33}^L}{V_{tb}V_{ts}^*} \right|^2, \quad (4.10)$$

where $a = \sqrt{2}\pi^2 / (e^2 G_F |C_L^{\text{SM}}|)$ with $C_L^{\text{SM}} \approx -6.38$ [32]. We use this constraint in our analysis and find that it significantly restricts our parameter space. Note that this constraint is applicable for λ_{23}^L and λ_{33}^L but not for λ_{23}^R .

4.4 Constraint from $Z \rightarrow \tau\tau$ decay

Another important constraint comes from the $Z\tau\tau$ coupling measurements. The $Z \rightarrow \tau\tau$ decay can be affected by the S_1 loops as shown in Ref. [47]. It is shown there that the major contribution of S_1 to the $Z\tau\tau$ coupling shift ($\Delta\kappa_{Z\tau\tau}$) comes when $S_1 t\tau$ coupling is large since the dominant part of $\Delta\kappa_{Z\tau\tau}$ is proportional to m_t^2 . Therefore, $Z\tau\tau$ coupling measurements can restrict only λ_{33}^L direction and almost blind to the λ_{23}^L direction. For instance, from Ref. [47], the $\lambda_{33}^L \gtrsim 1.4$ is excluded for $M_{S_1} \sim 1$ TeV with 2σ confidence limit.

4.5 LHC Phenomenology and constraints

Before discussing the LHC constraints, we make a quick survey of the relevant LHC phenomenology of a TeV range S_1 that couples with τ , ν and s - and c -quarks. For this discussion we compute all the necessary cross sections using the Universal FeynRules Output (UFO) [89] model files from Ref. [48] in MADGRAPH5 [90]. We use the NNPDF23LO [91] Parton Distribution Functions (PDFs). Wherever required, we include next-to-leading order QCD K -factor of ~ 1.3 for the pair production in our analysis [92].

4.5.1 Decay modes of S_1

In a situation where λ_{23}^L , λ_{33}^L and λ_{23}^R are nonzero, S_1 can decay to $c\tau$, $s\nu$, $t\tau$ and $b\nu$ modes. Due to the CKM mixing, decays to $u\tau$ and $d\nu$ will also arise. But we neglect them in our analysis since they are heavily suppressed by the small off-diagonal CKM elements. The BRs of S_1 to various decay modes vary depending on the coupling strengths. In case for $\lambda_{23}^R \gg \lambda_{23}^L, \lambda_{33}^L$, the dominant decay mode is $S_1 \rightarrow c\tau$. Whereas for $\lambda_{23}^L \gg \lambda_{23}^R, \lambda_{33}^L$ case, $\text{BR}(S_1 \rightarrow c\tau), \text{BR}(S_1 \rightarrow s\nu) \sim 50\%$. On the other hand, when $\lambda_{33}^L \gg \lambda_{23}^L, \lambda_{23}^R$, the dominant decay modes are $S_1 \rightarrow t\tau$ and $S_1 \rightarrow b\nu$ and they both share about 50% BRs. Note that though the partial widths depends linearly on M_{S_1} , BRs are almost insensitive to the M_{S_1} choice as it cancels in the ratios.

4.5.2 Production of S_1

At the LHC, S_1 can be produced resonantly in pairs or singly (single productions) and non-resonantly through the indirect production (t -channel S_1 exchange process).

Pair production: The pair production of S_1 is dominated by the strong coupling and, therefore, it is almost model-independent. The mild model-dependence enters in the pair production through the t -channel lepton or neutrino exchange processes. However, the amplitude of those diagrams are proportional to λ^2 and generally suppressed for small λ values (for bigger M_{S_1} and large λ values, this part could be comparable to the model independent part of the pair production). Pair production is heavily phase-space suppressed for large M_{S_1} and we find that its contribution is very small in our recast analysis. Pair

production can be categorized into two types depending on their final states, symmetric - where both leptoquarks decay to same modes, asymmetric - where two leptoquarks decay to two different modes. These two types give rise to various novel final states as follows

Symmetric modes:

$$S_1 S_1 \rightarrow \widehat{c\tau} \widehat{c\tau} \equiv \tau\tau + 2j; \quad \widehat{t\tau} \widehat{t\tau} \equiv tt + \tau\tau; \quad \widehat{s\nu} \widehat{s\nu} \equiv 2j + \cancel{E}_T; \quad \widehat{b\nu} \widehat{b\nu} \equiv 2b + \cancel{E}_T.$$

Asymmetric modes:

$$S_1 S_1 \rightarrow \widehat{c\tau} \widehat{s\nu} \equiv \tau + 2j + \cancel{E}_T; \quad \widehat{c\tau} \widehat{b\nu} \equiv \tau + b + j + \cancel{E}_T; \quad \widehat{c\tau} \widehat{t\tau} \equiv \tau\tau + t + j, \\ S_1 S_1 \rightarrow \widehat{s\nu} \widehat{b\nu} \equiv b + j + \cancel{E}_T; \quad \widehat{s\nu} \widehat{t\tau} \equiv t + \tau + j + \cancel{E}_T; \quad \widehat{b\nu} \widehat{t\tau} \equiv t + \tau + b + \cancel{E}_T,$$

where the curved connection over a pair of particles indicates that the pair is coming from a decay of S_1 . Searches for leptoquarks in some of the symmetric modes are already done at the LHC [85, 86]. Leptoquark searches in some of the symmetric and most of the asymmetric modes are yet to be performed at the LHC.

Single production: The single productions of S_1 , where S_1 is produced in association with a SM particle, are fully model dependent as they depend on the leptoquark-quark-lepton couplings. These are important production modes for large couplings and heavier masses, since single productions are less phase-space suppressed compared to pair production for heavier leptoquark masses. Depending on the final states, single productions can be categorized into the following categories.

Symmetric modes:

$$S_1 \tau X \rightarrow \widehat{\tau c} \tau + \widehat{\tau c} \tau j \quad (+ \widehat{\tau c} \tau jj + \dots) \equiv \tau\tau + jets \\ S_1 \tau X \rightarrow \widehat{\tau t} \tau + \widehat{\tau t} \tau j \quad (+ \widehat{\tau t} \tau jj + \dots) \equiv \tau\tau + t + jets \\ S_1 \nu X \rightarrow \widehat{\nu s} \nu + \widehat{\nu s} \nu j \quad (+ \widehat{\nu s} \nu jj + \dots) \equiv \cancel{E}_T + jets \\ S_1 \nu X \rightarrow \widehat{\nu b} \nu + \widehat{\nu b} \nu j \quad (+ \widehat{\nu b} \nu jj + \dots) \equiv \cancel{E}_T + b + jets$$

Asymmetric modes:

$$S_1 \tau X \rightarrow \widehat{\nu s} \tau + \widehat{\nu s} \tau j \quad (+ \widehat{\nu s} \tau jj + \dots) \equiv \cancel{E}_T + \tau + jets \\ S_1 \nu X \rightarrow \widehat{\tau c} \nu + \widehat{\tau c} \nu j \quad (+ \widehat{\tau c} \nu jj + \dots) \equiv \cancel{E}_T + \tau + jets \\ S_1 \tau X \rightarrow \widehat{\nu b} \tau + \widehat{\nu b} \tau j \quad (+ \widehat{\nu b} \tau jj + \dots) \equiv \cancel{E}_T + \tau + b + jets \\ S_1 \nu X \rightarrow \widehat{\tau t} \nu + \widehat{\tau t} \nu j \quad (+ \widehat{\tau t} \nu jj + \dots) \equiv \cancel{E}_T + \tau + t + jets$$

Here j stands for an untagged jet and $jets$ means any number (≥ 1) of untagged jets. These extra jets can be either radiation or hard (genuine three-body single production processes can have sizeable cross sections, see Refs. [93–95] for how one can systematically compute them). As single production is model dependent, the relative strengths of these modes with depend on the relative strengths of the coupling involved in the production as well as the BR of the decay mode involved.

Indirect production: Indirect production is the non-resonant process where a leptoquark is exchanged in the t -channel. With leptoquark couplings to τ and ν , this basically gives rise to three possible final states: $\tau\tau$ ($\tau\tau + jets$), $\tau\nu$ ($\cancel{E}_T + \tau + jets$) and $\nu\nu$ ($\cancel{E}_T + jets$). The amplitudes of these processes are proportional to λ^2 . So the cross section grows as λ^4 . Hence, for order one λ , the indirect production have larger cross section than other production processes for large M_{S_1} (see Fig. 2 of Ref. [48]). However, the indirect production substantially interfere with the SM background process $pp \rightarrow V^{(*)} \rightarrow \ell\ell$ ($\ell = \tau/\nu$). Though the interference is $\mathcal{O}(\lambda^2)$, its contribution can be significant for a TeV scale S_1 because of the large SM contribution (larger than both the direct production modes and the λ^4 indirect contribution, assuming $\lambda \gtrsim 1$). In general, the interference could be both constructive or destructive depending on the nature of the leptoquark species and its mass [96]. For S_1 , we find the interference is destructive in nature [48]. Hence, for a TeV scale S_1 if λ is large, this destructive interference becomes its dominant signature in the leptonic final states.

4.5.3 Constraints from the LHC

The mass exclusion limits from the pair production searches for S_1 at the LHC are as follows. Assuming 100% BR in the $S \rightarrow t\tau$ mode, a recent search at the CMS detector has excluded masses below 900 GeV [85]. Similarly, for a leptoquark that decays exclusively to $b\nu$ or $s\nu$ ($\equiv j\nu$) final states, the exclusion limits are at 1100 and 980 GeV [86], respectively. However, going beyond simple mass exclusions, we make use of the analysis done in Ref. [48] for the LHC constraints. It contains the independent LHC limits on the three couplings shown in Eq. 4.1 as functions of M_{S_1} as well as a summary of the direct detection exclusion limits.

Apart from the processes with $\cancel{E}_T + jets$ final states, all other production processes can have either $\tau\tau + jets$ final states or $\cancel{E}_T + \tau + jets$ final states. Hence, the latest $pp \rightarrow Z' \rightarrow \tau\tau$ and $pp \rightarrow W' \rightarrow \tau\nu$ searches at the ATLAS [97, 98] were used to derive the constraints in Ref. [48]. There we notice that the limits on λ_{23}^L from the $\tau\nu$ data are weaker than the ones obtained from the $\tau\tau$ data. The $\tau\tau$ data also constrain λ_{23}^R . From the earlier discussion, it is clear that the interference contribution plays the dominant role in determining these limits. However, its destructive nature means that in the signal region one would expect less events than the SM only predictions. Hence, the limits were obtained assuming either λ_{23}^L or λ_{23}^R is non-zero at a time and by performing a χ^2 test of the transverse mass (m_T) distributions of the data. As, for heavy S_1 , the limits on λ_{23}^L and λ_{23}^R are dominantly determined by the interference of the indirect production, they are very similar. We can translate these limits from the $\tau\tau$ data on any combination of λ_{23}^L and λ_{23}^R in a simple manner assuming $\lambda_{23}^{L/R} = \sqrt{(\lambda_{23}^L)^2 + (\lambda_{23}^R)^2}$. In Fig. 4 we display the limits on $\lambda_{23}^{L/R}$ as a function of M_{S_1} .⁴ Finally, the two searches in the $\tau\tau$ and $\tau + \cancel{E}_T$ channels are blind to λ_{33}^L because of the small b -PDF or the non existent t -PDF. Hence, λ_{33}^L remains unbounded from these searches.

⁴Actually, for M_{S_1} between 1 and 2 TeV, the limits on λ_{23}^L are slightly stronger than those on λ_{23}^R because in the SM the Z boson couples differently to left and right handed τ 's. However, we ignore this minor difference and take the stronger limits on λ_{23}^L as the limits on $\lambda_{23}^{L/R}$ to remain conservative.

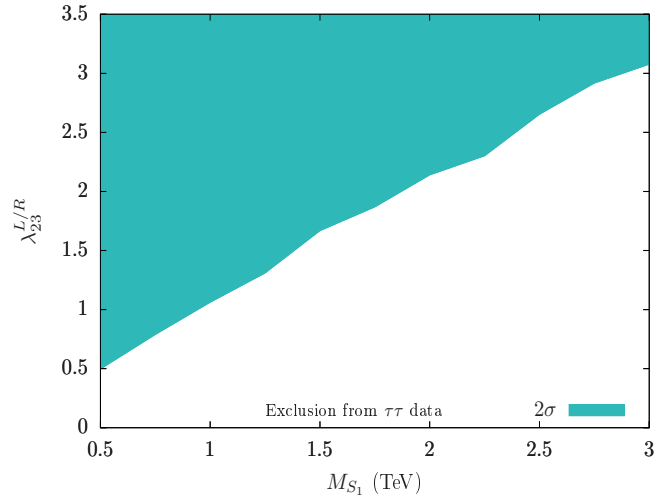


Figure 4. Two sigma exclusion limits on $\lambda_{23}^{L/R} = \sqrt{(\lambda_{23}^L)^2 + (\lambda_{23}^R)^2}$ as a function of M_{S_1} as obtained in Ref. [48] from the ATLAS $pp \rightarrow \tau\tau$ data [97]. The coloured region is excluded.

4.6 Parameter scan

To find the $R_{D^{(*)}}$ favoured regions in the S_1 parameter space that is not in conflict with the limit on $R_K^{\nu\nu}$, the observed $Z \rightarrow \tau\tau$ decay and the bounds from the LHC, we consider two benchmark leptoquark masses, $M_{S_1} = 1$ and 2 TeV. We allow all the three free couplings, λ_{23}^L , λ_{23}^R and λ_{33}^L to vary. For every benchmark mass, we perform a random scan over the three couplings in the range $-\sqrt{4\pi}$ to $\sqrt{4\pi}$ (i.e., $|\lambda|^2/4\pi \leq 1$). In this paper we do not consider complex values for the couplings. In Fig. 5, we show the outcome of our scan with different two dimensional projections. In every plot we show two couplings and allow the third coupling to vary (i.e., the third coupling is integrated out). In each of these plots we show

- **The *Flavour (F) regions*:** the blue dots marking the regions favoured by the $R_{D^{(*)}}$ observables within 95% CL while keeping $R_K^{\nu\nu} < 4.3$, the value obtained at 90% CL [88].
- **The *Flavour+EW (FEW) regions*:** In addition to the above flavour constraints, if we also consider the bounds on λ_{33}^L coming from the $Z \rightarrow \tau\tau$ decay within 95% CL [47], we get the regions marked by the green dots.
- **The *Flavour+EW+LHC (FEWL) regions*:** Finally, we get the regions marked by the red points when we take into account the limits on $\lambda_{23}^{L/R}$ from the ATLAS $pp \rightarrow \tau\tau$ data from the 13 TeV LHC [48] along with the previous constraints. These are the points that survive all the limits considered in this paper.

We show the *FEWL*-regions with magnification in Fig. 6. While considering these plots one has to keep in mind the following points.

- For the benchmark points chosen, the LHC puts bounds only on $\lambda_{23}^{L/R}$, not on λ_{33}^L whereas the $Z \rightarrow \tau\tau$ data puts bounds only on λ_{33}^L ; making these two constraints

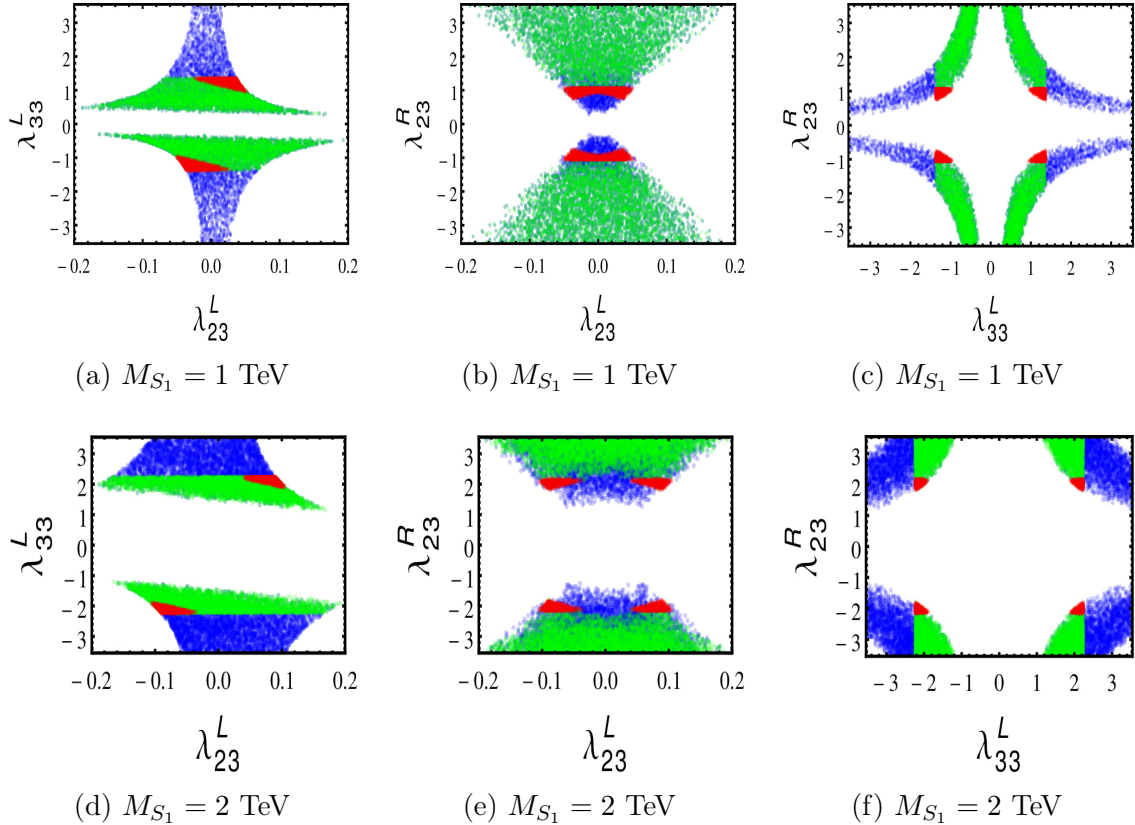


Figure 5. Two dimensional projections of the regions in the S_1 parameter space allowed by (i) the flavour observables alone - the F -regions (blue), (ii) the flavour observables and the $Z \rightarrow \tau\tau$ decay - the FEW -regions (green) and (iii) the flavour observables, the $Z \rightarrow \tau\tau$ decay and the LHC constraints - the $FEWL$ -regions (red) for $M_{S_1} = 1$ TeV (upper panel) and $M_{S_1} = 2$ TeV (lower panel). We assume all the couplings to be real. The $FEWL$ -regions are shown separately in Fig. 6.

complimentary to each other. This can be seen from Fig. 5 – the green regions have upper boundaries in $|\lambda_{33}^L|$.

- To explain only the $R_{D^{(*)}}$ anomalies either λ_{23}^L or λ_{33}^L could be large while keeping the other two couplings small [48]. But, generally, a big λ_{23}^L gets into conflict with $R_K^{\nu\nu}$ and is also independently constrained by the LHC data [48] whereas a big λ_{33}^L is restricted by the $Z \rightarrow \tau\tau$ decay [47].
- The LHC data also restricts a scenario with large λ_{23}^R and a small λ_{23}^L .

From Fig. 6 we see that when all the constraints are put together, they prefer a small λ_{23}^L but push both λ_{23}^R and λ_{33}^L to higher values. The actual values increase with increasing M_{S_1} as the leptoquark contributions to all these processes decrease with increasing mass and hence larger couplings are required to compensate this fall.

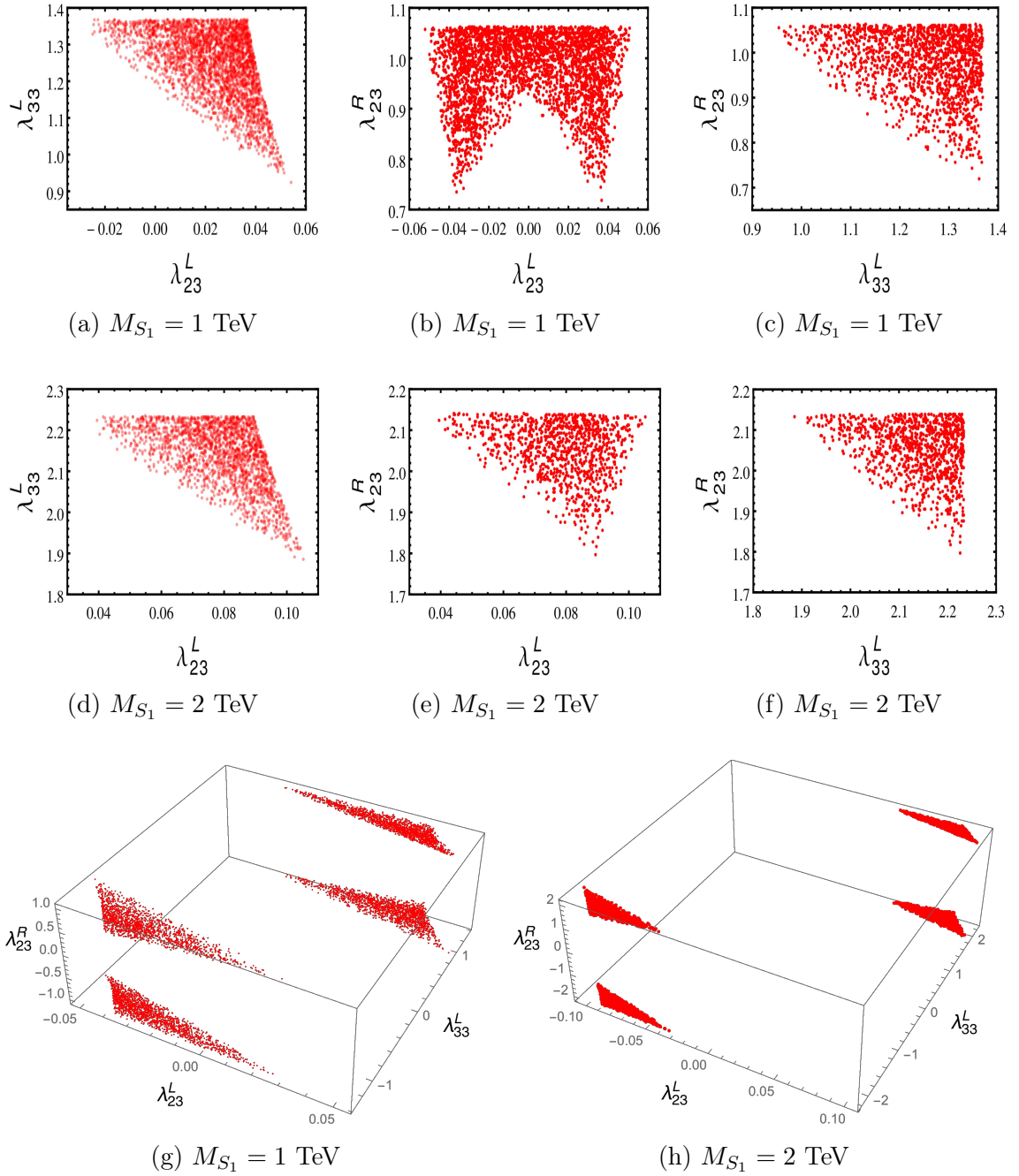


Figure 6. The *FEWL*-regions (the regions in the S_1 parameter space allowed by the flavour observables, the $Z \rightarrow \tau\tau$ decay and the LHC constraints) from Fig. 5 shown separately. The two-dimensional projections of the *FEWL*-regions for $M_{S_1} = 1$ ($M_{S_1} = 2$) TeV are shown after magnification in the upper panel (middle panel). In the lower panel we show these regions in 3D plots for clarity.

5 Discussion and conclusions

In this paper, we consider the scenario that there is a single scalar leptoquark, S_1 , at the TeV-scale, and it is the colour-triplet component of a real $\mathbf{10}$ of $\text{SO}(10)$, which also contains a $\text{SU}(2)$ doublet which is identified as the SM Higgs. In this scenario, the leptoquark being the only scalar entity other than the SM Higgs is natural; peculiar mass-splitting between the components of $\mathbf{10}$ does not occur and the leptoquark picks up an electroweak-scale mass together with the SM Higgs, as expected. This is appealing because this leptoquark by itself can potentially explain the B -decay anomalies at the LHC [21, 22, 25, 32].

The $\text{SO}(10)$ grand unification framework is an appealing scenario, which has been heavily studied in the literature [60, 62–73]. It unifies the three forces in the SM, explains the quantization of electric charge, provides numerous dark matter candidates, accommodates see-saw mechanism for small neutrino masses, and justifies the remarkable cancellation of anomalies through the anomaly-free nature of the $\text{SO}(10)$ gauge group. Moreover, the fermionic content of the SM fits elegantly in $\mathbf{16}_F$, including a right-handed neutrino for each family. Furthermore, the fermion content of the SM possesses masses up to the electroweak scale in varying degrees of magnitude, consistent with the electroweak-scale Higgs field, which is generally assigned to a real $\mathbf{10}_H$. Considering that the leptoquark S_1 is the only other component in $\mathbf{10}_H$, a TeV-scale S_1 , from this perspective, is consistent with the idea that it is the last piece of the puzzle regarding the particle content up to the electroweak scale (modulo the right-handed neutrinos). Therefore, possible detection of S_1 , in absence of any other new particles, at the TeV-scale could be interpreted as an evidence in favour of $\text{SO}(10)$ grand unification.

One obvious issue for concern is proton decay since the leptoquark S_1 possesses the right quantum numbers for it to couple to potentially dangerous diquark operators. On the other hand, the proton stability could possibly be ensured through various mechanisms [22, 38, 66, 74–76]. In this paper, we ensure the proton stability by turning off these couplings. However, we do not address possible underlying reasons behind the suppression or the elimination of these terms. This does not affect our analysis regarding the LHC searches since they should not be there anyway due to the apparent stability of proton and it does not affect the gauge coupling unification since these couplings do not play role in the one-loop RG running.

Having a single S_1 leptoquark at TeV-scale as the only new physics remnant from our $\text{SO}(10)$ GUT model, we investigate how competent this S_1 is to address the $R_{D^{(*)}}$ anomalies while simultaneously satisfying other relevant constraints from flavour, electroweak and the direct LHC searches. We adopt a specific Yukawa coupling texture with only three free (real) nonzero couplings viz. λ_{23}^L , λ_{33}^L and λ_{23}^R . We have found that this minimal consideration can alleviate the potential tension between the $R_{D^{(*)}}$ -favoured region and the $R_K^{\nu\nu}$ measurements. The $Z \rightarrow \tau\tau$ decay measurements is very powerful to constrain λ_{33}^L whereas the $\tau\tau$ resonance search data from the LHC restrict the λ_{23}^L and λ_{23}^R couplings. By combining all these constrains, we have found that a tiny region of the $R_{D^{(*)}}$ -favoured parameter space is still allowed. We observe that among all these constraints, the latest LHC $\tau\tau$ resonance search data is the most powerful one to restrict the parameter space of

our economic set-up. Evidently, by introducing new degrees of freedom in our framework, one can, a priori, enlarge the allowed parameter region. For example, by considering some of the couplings complex or by choosing a complex **10** (instead of a real) representation of SO(10), which will introduce an additional S_1 and another complex scalar doublet at the TeV-scale, one can relax our obtained bounds. We also point out search strategies of S_1 at the LHC using symmetric and asymmetric pair and single production channels. Systematic studies of these channels is beyond the scope of this paper and can be discussed elsewhere.

Acknowledgements

We thank Diganta Das for valuable discussions and collaborating in the initial part of the project. U.A. is supported by the National Natural Science Foundation of China (NSFC) under Grant No. 11505067. T.M. is financially supported by the Royal Society of Arts and Sciences of Uppsala as a researcher at Uppsala University and by the INSPIRE Faculty Fellowship of the Department of Science and Technology (DST) under grant number IFA16-PH182 at the University of Delhi. S.M. acknowledges support from the Science and Engineering Research Board (SERB), DST, India under grant number ECR/2017/000517.

References

- [1] BaBar collaboration, J. P. Lees et al., *Evidence for an excess of $\bar{B} \rightarrow D^{(*)}\tau^-\bar{\nu}_\tau$ decays*, *Phys. Rev. Lett.* **109** (2012) 101802, [[1205.5442](#)].
- [2] BaBar collaboration, J. P. Lees et al., *Measurement of an Excess of $\bar{B} \rightarrow D^{(*)}\tau^-\bar{\nu}_\tau$ Decays and Implications for Charged Higgs Bosons*, *Phys. Rev.* **D88** (2013) 072012, [[1303.0571](#)].
- [3] LHCb collaboration, R. Aaij et al., *Test of lepton universality using $B^+ \rightarrow K^+\ell^+\ell^-$ decays*, *Phys. Rev. Lett.* **113** (2014) 151601, [[1406.6482](#)].
- [4] LHCb collaboration, R. Aaij et al., *Test of lepton universality with $B^0 \rightarrow K^{*0}\ell^+\ell^-$ decays*, *JHEP* **08** (2017) 055, [[1705.05802](#)].
- [5] LHCb collaboration, R. Aaij et al., *Measurement of the ratio of branching fractions $\mathcal{B}(\bar{B}^0 \rightarrow D^{*+}\tau^-\bar{\nu}_\tau)/\mathcal{B}(\bar{B}^0 \rightarrow D^{*+}\mu^-\bar{\nu}_\mu)$* , *Phys. Rev. Lett.* **115** (2015) 111803, [[1506.08614](#)].
- [6] LHCb collaboration, R. Aaij et al., *Measurement of the ratio of the $B^0 \rightarrow D^{*-}\tau^+\nu_\tau$ and $B^0 \rightarrow D^{*-}\mu^+\nu_\mu$ branching fractions using three-prong τ -lepton decays*, *Phys. Rev. Lett.* **120** (2018) 171802, [[1708.08856](#)].
- [7] LHCb collaboration, R. Aaij et al., *Test of Lepton Flavor Universality by the measurement of the $B^0 \rightarrow D^{*-}\tau^+\nu_\tau$ branching fraction using three-prong τ decays*, *Phys. Rev.* **D97** (2018) 072013, [[1711.02505](#)].
- [8] Belle collaboration, M. Huschle et al., *Measurement of the branching ratio of $\bar{B} \rightarrow D^{(*)}\tau^-\bar{\nu}_\tau$ relative to $\bar{B} \rightarrow D^{(*)}\ell^-\bar{\nu}_\ell$ decays with hadronic tagging at Belle*, *Phys. Rev.* **D92** (2015) 072014, [[1507.03233](#)].
- [9] Belle collaboration, Y. Sato et al., *Measurement of the branching ratio of $\bar{B}^0 \rightarrow D^{*+}\tau^-\bar{\nu}_\tau$ relative to $\bar{B}^0 \rightarrow D^{*+}\ell^-\bar{\nu}_\ell$ decays with a semileptonic tagging method*, *Phys. Rev.* **D94** (2016) 072007, [[1607.07923](#)].

- [10] Belle collaboration, S. Hirose et al., *Measurement of the τ lepton polarization and $R(D^*)$ in the decay $\bar{B} \rightarrow D^* \tau^- \bar{\nu}_\tau$* , *Phys. Rev. Lett.* **118** (2017) 211801, [[1612.00529](#)].
- [11] Belle collaboration, S. Hirose et al., *Measurement of the τ lepton polarization and $R(D^*)$ in the decay $\bar{B} \rightarrow D^* \tau^- \bar{\nu}_\tau$ with one-prong hadronic τ decays at Belle*, *Phys. Rev.* **D97** (2018) 012004, [[1709.00129](#)].
- [12] D. Bigi and P. Gambino, *Revisiting $B \rightarrow D \ell \nu$* , *Phys. Rev.* **D94** (2016) 094008, [[1606.08030](#)].
- [13] F. U. Bernlochner, Z. Ligeti, M. Papucci and D. J. Robinson, *Combined analysis of semileptonic B decays to D and D^* : $R(D^{(*)})$, $|V_{cb}|$, and new physics*, *Phys. Rev.* **D95** (2017) 115008, [[1703.05330](#)].
- [14] D. Bigi, P. Gambino and S. Schacht, *$R(D^*)$, $|V_{cb}|$, and the Heavy Quark Symmetry relations between form factors*, *JHEP* **11** (2017) 061, [[1707.09509](#)].
- [15] S. Jaiswal, S. Nandi and S. K. Patra, *Extraction of $|V_{cb}|$ from $B \rightarrow D^{(*)} \ell \nu_\ell$ and the Standard Model predictions of $R(D^{(*)})$* , *JHEP* **12** (2017) 060, [[1707.09977](#)].
- [16] Heavy Flavor Averaging Group, *Average of R_D and R_{D^*} for FPCCP 2017*, .
- [17] G. Hiller and F. Kruger, *More model-independent analysis of $b \rightarrow s$ processes*, *Phys. Rev.* **D69** (2004) 074020, [[hep-ph/0310219](#)].
- [18] M. Bordone, G. Isidori and A. Pattori, *On the Standard Model predictions for R_K and R_{K^*}* , *Eur. Phys. J.* **C76** (2016) 440, [[1605.07633](#)].
- [19] I. Doršner, S. Fajfer, N. Košnik and I. Nišandžić, *Minimally flavored colored scalar in $\bar{B} \rightarrow D^{(*)} \tau \bar{\nu}$ and the mass matrices constraints*, *JHEP* **11** (2013) 084, [[1306.6493](#)].
- [20] Y. Sakaki, M. Tanaka, A. Tayduganov and R. Watanabe, *Testing leptoquark models in $\bar{B} \rightarrow D^{(*)} \tau \bar{\nu}$* , *Phys. Rev.* **D88** (2013) 094012, [[1309.0301](#)].
- [21] M. Freytsis, Z. Ligeti and J. T. Ruderman, *Flavor models for $\bar{B} \rightarrow D^{(*)} \tau \bar{\nu}$* , *Phys. Rev.* **D92** (2015) 054018, [[1506.08896](#)].
- [22] M. Bauer and M. Neubert, *Minimal Leptoquark Explanation for the $R_{D^{(*)}}$, R_K , and $(g-2)_\mu$ Anomalies*, *Phys. Rev. Lett.* **116** (2016) 141802, [[1511.01900](#)].
- [23] B. Dumont, K. Nishiwaki and R. Watanabe, *LHC constraints and prospects for S_1 scalar leptoquark explaining the $\bar{B} \rightarrow D^{(*)} \tau \bar{\nu}$ anomaly*, *Phys. Rev.* **D94** (2016) 034001, [[1603.05248](#)].
- [24] D. Das, C. Hati, G. Kumar and N. Mahajan, *Towards a unified explanation of $R_{D^{(*)}}$, R_K and $(g-2)_\mu$ anomalies in a left-right model with leptoquarks*, *Phys. Rev.* **D94** (2016) 055034, [[1605.06313](#)].
- [25] D. Bečirević, N. Košnik, O. Sumensari and R. Zukanovich Funchal, *Palatable Leptoquark Scenarios for Lepton Flavor Violation in Exclusive $b \rightarrow s \ell_1 \ell_2$ modes*, *JHEP* **11** (2016) 035, [[1608.07583](#)].
- [26] D. Bečirević, S. Fajfer, N. Košnik and O. Sumensari, *Leptoquark model to explain the B -physics anomalies, R_K and R_D* , *Phys. Rev.* **D94** (2016) 115021, [[1608.08501](#)].
- [27] D. A. Faroughy, A. Greljo and J. F. Kamenik, *Confronting lepton flavor universality violation in B decays with high- p_T tau lepton searches at LHC*, *Phys. Lett.* **B764** (2017) 126–134, [[1609.07138](#)].
- [28] G. Hiller, D. Loose and K. Schönwald, *Leptoquark Flavor Patterns & B Decay Anomalies*, *JHEP* **12** (2016) 027, [[1609.08895](#)].

- [29] C.-H. Chen, T. Nomura and H. Okada, *Excesses of muon $g - 2$, $R_{D^{(*)}}$, and R_K in a leptoquark model*, *Phys. Lett.* **B774** (2017) 456–464, [[1703.03251](#)].
- [30] A. Crivellin, D. Müller and T. Ota, *Simultaneous explanation of $R(D^{(*)})$ and $b \rightarrow s\mu^+\mu^-$: the last scalar leptoquarks standing*, *JHEP* **09** (2017) 040, [[1703.09226](#)].
- [31] D. Bečirević and O. Sumensari, *A leptoquark model to accommodate $R_K^{\text{exp}} < R_K^{\text{SM}}$ and $R_{K^*}^{\text{exp}} < R_{K^*}^{\text{SM}}$* , *JHEP* **08** (2017) 104, [[1704.05835](#)].
- [32] Y. Cai, J. Gargalionis, M. A. Schmidt and R. R. Volkas, *Reconsidering the One Leptoquark solution: flavor anomalies and neutrino mass*, *JHEP* **10** (2017) 047, [[1704.05849](#)].
- [33] W. Altmannshofer, P. Bhupal Dev and A. Soni, *$R_{D^{(*)}}$ anomaly: A possible hint for natural supersymmetry with R -parity violation*, *Phys. Rev.* **D96** (2017) 095010, [[1704.06659](#)].
- [34] N. Assad, B. Fornal and B. Grinstein, *Baryon Number and Lepton Universality Violation in Leptoquark and Diquark Models*, *Phys. Lett.* **B777** (2018) 324–331, [[1708.06350](#)].
- [35] M. Jung and D. M. Straub, *Constraining new physics in $b \rightarrow c\ell\nu$ transitions*, *JHEP* **01** (2019) 009, [[1801.01112](#)].
- [36] A. Biswas, D. K. Ghosh, S. K. Patra and A. Shaw, *$b \rightarrow c\ell\nu$ anomalies in light of extended scalar sectors*, [[1801.03375](#)].
- [37] P. Bandyopadhyay and R. Mandal, *Revisiting scalar leptoquark at the LHC*, *Eur. Phys. J.* **C78** (2018) 491, [[1801.04253](#)].
- [38] U. Aydemir, D. Minic, C. Sun and T. Takeuchi, *B -decay anomalies and scalar leptoquarks in unified Pati-Salam models from noncommutative geometry*, *JHEP* **09** (2018) 117, [[1804.05844](#)].
- [39] D. Marzocca, *Addressing the B -physics anomalies in a fundamental Composite Higgs Model*, *JHEP* **07** (2018) 121, [[1803.10972](#)].
- [40] D. Bečirević, I. Doršner, S. Fajfer, N. Košnik, D. A. Faroughy and O. Sumensari, *Scalar leptoquarks from grand unified theories to accommodate the B -physics anomalies*, *Phys. Rev.* **D98** (2018) 055003, [[1806.05689](#)].
- [41] J. Kumar, D. London and R. Watanabe, *Combined Explanations of the $b \rightarrow s\mu^+\mu^-$ and $b \rightarrow c\tau^-\bar{\nu}$ Anomalies: a General Model Analysis*, *Phys. Rev.* **D99** (2019) 015007, [[1806.07403](#)].
- [42] Q.-Y. Hu, X.-Q. Li, Y. Muramatsu and Y.-D. Yang, *R -parity violating solutions to the $R_{D^{(*)}}$ anomaly and their GUT -scale unifications*, *Phys. Rev.* **D99** (2019) 015008, [[1808.01419](#)].
- [43] T. Faber, M. Hudec, M. Malinský, P. Meinzinger, W. Porod and F. Staub, *A unified leptoquark model confronted with lepton non-universality in B -meson decays*, *Phys. Lett.* **B787** (2018) 159–166, [[1808.05511](#)].
- [44] J. Heeck and D. Teresi, *Pati-Salam explanations of the B -meson anomalies*, *JHEP* **12** (2018) 103, [[1808.07492](#)].
- [45] A. Angelescu, D. Bečirević, D. A. Faroughy and O. Sumensari, *Closing the window on single leptoquark solutions to the B -physics anomalies*, *JHEP* **10** (2018) 183, [[1808.08179](#)].
- [46] S. Bifani, S. Descotes-Genon, A. Romero Vidal and M.-H. Schune, *Review of Lepton Universality tests in B decays*, *J. Phys.* **G46** (2019) 023001, [[1809.06229](#)].
- [47] S. Bansal, R. M. Capdevilla and C. Kolda, *On the Minimal Flavor Violating Leptoquark Explanation of the $R_{D^{(*)}}$ Anomaly*, [[1810.11588](#)].

- [48] T. Mandal, S. Mitra and S. Raz, $R_{D^{(*)}}$ in minimal leptoquark scenarios: impact of interference on the exclusion limits from LHC data, [1811.03561](#).
- [49] S. Iguro, T. Kitahara, R. Watanabe and K. Yamamoto, D^* polarization vs. $R_{D^{(*)}}$ anomalies in the leptoquark models, [1811.08899](#).
- [50] J. Aebischer, A. Crivellin and C. Greub, QCD Improved Matching for Semi-Leptonic B Decays with Leptoquarks, [1811.08907](#).
- [51] S. Bar-Shalom, J. Cohen, A. Soni and J. Wudka, Phenomenology of TeV-scale scalar Leptoquarks in the EFT, [1812.03178](#).
- [52] T. J. Kim, P. Ko, J. Li, J. Park and P. Wu, Correlation between $R_{D^{(*)}}$ and top quark FCNC decays in leptoquark models, [1812.08484](#).
- [53] B. Bhattacharya, A. Datta, J.-P. Guévin, D. London and R. Watanabe, Simultaneous Explanation of the R_K and $R_{D^{(*)}}$ Puzzles: a Model Analysis, *JHEP* **01** (2017) 015, [[1609.09078](#)].
- [54] S. Sahoo and R. Mohanta, Impact of vector leptoquark on $\bar{B} \rightarrow \bar{K}^* l^+ l^-$ anomalies, *J. Phys.* **G45** (2018) 085003, [[1806.01048](#)].
- [55] A. Crivellin, C. Greub, D. Muller and F. Saturnino, Importance of Loop Effects in Explaining the Accumulated Evidence for New Physics in B Decays with a Vector Leptoquark, *Phys. Rev. Lett.* **122** (2019) 011805, [[1807.02068](#)].
- [56] A. Biswas, D. Kumar Ghosh, N. Ghosh, A. Shaw and A. K. Swain, Novel collider signature of U_1 Leptoquark and $B \rightarrow \pi$ observables, [1808.04169](#).
- [57] S. Balaji, R. Foot and M. A. Schmidt, A chiral $SU(4)$ explanation of the $b \rightarrow s$ anomalies, *Phys. Rev.* **D99** (2019) 015029, [[1809.07562](#)].
- [58] A. Biswas, A. K. Swain and A. Shaw, Collider signature of V_2 Leptoquark with $b \rightarrow s$ flavour observables, [1811.08887](#).
- [59] B. Fornal, S. A. Gadam and B. Grinstein, Left-Right $SU(4)$ Vector Leptoquark Model for Flavor Anomalies, [1812.01603](#).
- [60] H. Fritzsch and P. Minkowski, Unified Interactions of Leptons and Hadrons, *Annals Phys.* **93** (1975) 193–266.
- [61] H. Georgi, The State of the Art–Gauge Theories, *AIP Conf. Proc.* **23** (1975) 575–582.
- [62] D. Chang, R. N. Mohapatra and M. K. Parida, Decoupling Parity and $SU(2)$ -R Breaking Scales: A New Approach to Left-Right Symmetric Models, *Phys. Rev. Lett.* **52** (1984) 1072.
- [63] D. Chang, R. N. Mohapatra and M. K. Parida, A New Approach to Left-Right Symmetry Breaking in Unified Gauge Theories, *Phys. Rev.* **D30** (1984) 1052.
- [64] D. Chang, R. N. Mohapatra, J. Gipson, R. E. Marshak and M. K. Parida, Experimental Tests of New $SO(10)$ Grand Unification, *Phys. Rev.* **D31** (1985) 1718.
- [65] N. G. Deshpande, E. Keith and P. B. Pal, Implications of LEP results for $SO(10)$ grand unification, *Phys. Rev.* **D46** (1993) 2261–2264.
- [66] B. Bajc, A. Melfo, G. Senjanovic and F. Vissani, Yukawa sector in non-supersymmetric renormalizable $SO(10)$, *Phys. Rev.* **D73** (2006) 055001, [[hep-ph/0510139](#)].
- [67] S. Bertolini, L. Di Luzio and M. Malinsky, Intermediate mass scales in the

- non-supersymmetric SO(10) grand unification: A Reappraisal*, *Phys. Rev.* **D80** (2009) 015013, [[0903.4049](#)].
- [68] K. S. Babu and R. N. Mohapatra, *Coupling Unification, GUT-Scale Baryogenesis and Neutron-Antineutron Oscillation in SO(10)*, *Phys. Lett.* **B715** (2012) 328–334, [[1206.5701](#)].
- [69] G. Altarelli and D. Meloni, *A non supersymmetric SO(10) grand unified model for all the physics below M_{GUT}* , *JHEP* **08** (2013) 021, [[1305.1001](#)].
- [70] U. Aydemir, *SO(10) grand unification in light of recent LHC searches and colored scalars at the TeV-scale*, *Int. J. Mod. Phys.* **A31** (2016) 1650034, [[1512.00568](#)].
- [71] U. Aydemir and T. Mandal, *LHC probes of TeV-scale scalars in SO(10) grand unification*, *Adv. High Energy Phys.* **2017** (2017) 7498795, [[1601.06761](#)].
- [72] K. S. Babu and S. Khan, *Minimal nonsupersymmetric SO(10) model: Gauge coupling unification, proton decay, and fermion masses*, *Phys. Rev.* **D92** (2015) 075018, [[1507.06712](#)].
- [73] K. S. Babu, B. Bajc and S. Saad, *Yukawa Sector of Minimal SO(10) Unification*, *JHEP* **02** (2017) 136, [[1612.04329](#)].
- [74] P. Cox, A. Kusenko, O. Sumensari and T. T. Yanagida, *SU(5) Unification with TeV-scale Leptoquarks*, *JHEP* **03** (2017) 035, [[1612.03923](#)].
- [75] J. C. Pati and A. Salam, *Lepton Number as the Fourth Color*, *Phys. Rev.* **D10** (1974) 275–289.
- [76] G. R. Dvali, *Light color triplet Higgs is compatible with proton stability: An Alternative approach to the doublet - triplet splitting problem*, *Phys. Lett.* **B372** (1996) 113–120, [[hep-ph/9511237](#)].
- [77] A. Maiezza, M. Nemevsek, F. Nesti and G. Senjanovic, *Left-Right Symmetry at LHC*, *Phys. Rev.* **D82** (2010) 055022, [[1005.5160](#)].
- [78] P. Bandyopadhyay and R. Mandal, *Vacuum stability in an extended standard model with a leptoquark*, *Phys. Rev.* **D95** (2017) 035007, [[1609.03561](#)].
- [79] D. R. T. Jones, *The Two Loop beta Function for a $G(1) \times G(2)$ Gauge Theory*, *Phys. Rev.* **D25** (1982) 581.
- [80] M. Lindner and M. Weiser, *Gauge coupling unification in left-right symmetric models*, *Phys. Lett.* **B383** (1996) 405–414, [[hep-ph/9605353](#)].
- [81] Particle Data Group collaboration, C. Patrignani et al., *Review of Particle Physics*, *Chin. Phys.* **C40** (2016) 100001.
- [82] SLD Electroweak Group, DELPHI, ALEPH, SLD, SLD Heavy Flavour Group, OPAL, LEP Electroweak Working Group, L3 collaboration, S. Schael et al., *Precision electroweak measurements on the Z resonance*, *Phys. Rept.* **427** (2006) 257–454, [[hep-ex/0509008](#)].
- [83] Super-Kamiokande collaboration, K. Abe et al., *Search for proton decay via $p \rightarrow e^+\pi^0$ and $p \rightarrow \mu^+\pi^0$ in 0.31 megaton 7 years exposure of the Super-Kamiokande water Cherenkov detector*, *Phys. Rev.* **D95** (2017) 012004, [[1610.03597](#)].
- [84] P. Langacker, *Grand Unified Theories and Proton Decay*, *Phys. Rept.* **72** (1981) 185.
- [85] CMS collaboration, A. M. Sirunyan et al., *Search for third-generation scalar leptoquarks decaying to a top quark and a τ lepton at $\sqrt{s} = 13$ TeV*, *Eur. Phys. J.* **C78** (2018) 707, [[1803.02864](#)].

- [86] CMS collaboration, A. M. Sirunyan et al., *Constraints on models of scalar and vector leptoquarks decaying to a quark and a neutrino at $\sqrt{s} = 13$ TeV*, *Phys. Rev.* **D98** (2018) 032005, [[1805.10228](#)].
- [87] A. Celis, M. Jung, X.-Q. Li and A. Pich, *Scalar contributions to $b \rightarrow c(u)\tau\nu$ transitions*, *Phys. Lett.* **B771** (2017) 168–179, [[1612.07757](#)].
- [88] A. J. Buras, J. Girrbach-Noe, C. Niehoff and D. M. Straub, *$B \rightarrow K^{(*)}\nu\bar{\nu}$ decays in the Standard Model and beyond*, *JHEP* **02** (2015) 184, [[1409.4557](#)].
- [89] C. Degrande, C. Duhr, B. Fuks, D. Grellscheid, O. Mattelaer and T. Reiter, *UFO - The Universal FeynRules Output*, *Comput. Phys. Commun.* **183** (2012) 1201–1214, [[1108.2040](#)].
- [90] J. Alwall, R. Frederix, S. Frixione, V. Hirschi, F. Maltoni, O. Mattelaer et al., *The automated computation of tree-level and next-to-leading order differential cross sections, and their matching to parton shower simulations*, *JHEP* **07** (2014) 079, [[1405.0301](#)].
- [91] R. D. Ball et al., *Parton distributions with LHC data*, *Nucl. Phys.* **B867** (2013) 244–289, [[1207.1303](#)].
- [92] T. Mandal, S. Mitra and S. Seth, *Pair Production of Scalar Leptoquarks at the LHC to NLO Parton Shower Accuracy*, *Phys. Rev.* **D93** (2016) 035018, [[1506.07369](#)].
- [93] T. Mandal and S. Mitra, *Probing Color Octet Electrons at the LHC*, *Phys. Rev.* **D87** (2013) 095008, [[1211.6394](#)].
- [94] T. Mandal, S. Mitra and S. Seth, *Single Productions of Colored Particles at the LHC: An Example with Scalar Leptoquarks*, *JHEP* **07** (2015) 028, [[1503.04689](#)].
- [95] T. Mandal, S. Mitra and S. Seth, *Probing Compositeness with the CMS $eejj$ & eej Data*, *Phys. Lett.* **B758** (2016) 219–225, [[1602.01273](#)].
- [96] S. Bansal, R. M. Capdevilla, A. Delgado, C. Kolda, A. Martin and N. Raj, *Hunting leptoquarks in monolepton searches*, *Phys. Rev.* **D98** (2018) 015037, [[1806.02370](#)].
- [97] ATLAS collaboration, M. Aaboud et al., *Search for additional heavy neutral Higgs and gauge bosons in the ditau final state produced in 36 fb^{-1} of pp collisions at $\sqrt{s} = 13$ TeV with the ATLAS detector*, *JHEP* **01** (2018) 055, [[1709.07242](#)].
- [98] ATLAS collaboration, M. Aaboud et al., *Search for High-Mass Resonances Decaying to $\tau\nu$ in pp Collisions at $\sqrt{s} = 13$ TeV with the ATLAS Detector*, *Phys. Rev. Lett.* **120** (2018) 161802, [[1801.06992](#)].